Refreshable Tactile Display Based on a Bistable Electroactive Polymer and Stretchable Serpentine Joule Heating Electrode

*Yu Qiu, Zhiyun Lu, and Qibing Pei**

Department of Materials Science and Engineering, Henry Samueli School of Engineering and Applied Science, University of California, Los Angeles, CA 90095, USA

KEYWORDS: refreshable tactile display, bistable, variable stiffness, stretchable Joule heating, serpentine electrode

ABSTRACT: The demand for tactile interactive devices has been growing exponentially as the sense of touch enriches the human-machine interaction experience. However, tactile devices reported so far cannot offer high quality performance, compact form factor, and relatively simple system architecture for low cost production. We report the fabrication of a 4 × 4 pneumatic tactile display with Braille standard resolution using a bistable electroactive polymer thin film and serpentine-patterned carbon nanotube electrode. The bistable electroactive polymer is a variable stiffness material that exhibits stiffness change of 3000-fold within the narrow temperature range of 43 ± 3 ºC. The carbon nanotube electrode was patterned on the polymer film via a P3R process, Prestretch-Pattern-Protect-Release, which leads to a serpentine-patterned composite electrode that is highly stretchable, retains its high electrical conductivity up to ~200% area strain, and provides fast Joule heating rate of 31 ºC/s. The tactile pixels are diaphragm actuators that can be individually controlled to produce 0.7 mm out of plain deformation and greater than 50 g of blocking force by application of local heating and pneumatic pressure. The device can operate under low voltage

supply (30 V) and has a lifetime of over 100,000 cycles without much performance degradation. This work could open a path to building compact, user friendly, and cost-effective tactile devices for a variety of important applications.

1. INTRODUCTION

The interests in developing tactile interactive devices have been growing exponentially in recent years thanks to the increasing demands in a wide range of areas from virtual surgery training in medical technology[1–3], haptic controller of virtual reality (VR) headset in entertainment[4,5], and telemanipulation in robotic controls[6,7]. Tactile communication is also indispensable for people who are visually impaired[8]. Unlike audible and visual means, which are restricted to specific body parts, the sense of touch covers the entire body. Thus, by adding the sense of touch, the quality and amount of information one can gain from a machine will be substantially enriched. The most widely studied tactile displays are those that provide normal indentation to user's fingertips by vertically moving miniature pins to reproduce shape, pattern, or textures. Despite the growing needs, the critical technology barriers have resulted in a handful of tactile display products available on the market. In particular, there lacks a suitable actuation mechanism that can produce large deformations with sufficiently high blocking force, can be packaged at high pixel resolution, have compact form factor and light weight, and can be produced at low costs[9].

Most of the tactile devices suffer from bulky actuator structures. Piezoelectric bimorph tactile displays exhibit high blocking force at a wide frequency range[10,11]. Unfortunately, these devices are bulky due to the encumbrance of the cantilevers. Tactile shape display using RC servomotors[12] have large displacement and appropriate actuator density but are also bulky (76 mm × 76 mm × 119 mm) and inconvenient for day to day operation. Shape memory alloy (SMA)[13] have also been

implemented in previous tactile displays. The requirement for extensive heating and cooling steps limits the utility of the device, and raises manufacturing costs. Phase changing materials that exhibit volume change over melting[14] or boiling[15,16] point were developed as refreshable Braille cells. These devices, which require miniature Joule heating electrode and thermally insulated chamber for each dot, have complex architecture and usually exert small stroke and force.

In recent years, dielectric elastomer actuators (DEA) have emerged as a promising compact tactile display technology [17,18]. Their light weight, high actuator density, and high stroke range offered the same performance as previous technologies but in much more compact form factors. However, the translation of the DEA technology to marketplace has been sluggish, due to the high driving voltages which could cause static shocks or even injury. Attempts by researchers to incorporate insulating layers to seal the DEA generally lowered the actuation performance and increased the fabrication complexity.[19–23] We reported an alternative approach to fabricating a refreshable Braille display using a bistable electroactive polymer (BSEP) as an electroactive transducer. [24] The shape memory property of the BSEP allowed for separation of high voltage elements from operators, but the device used an external heater, and the resulting stroke was small. While mitigated in the BSEP designs, the concerns for high voltage were not eliminated entirety.

In comparison to the electric stimuli, pneumatic tactile devices are usually more stable and can provide higher force feedback. However, most pneumatic devices either have complex structures which require individual air streams for each actuator [25], or require electrostatic microvalves for each dot [26]. Scaling up the number of actuators while maintaining compact form factor is challenging. Recently, Besse et al.[27] reported a 32 by 24 actuator pneumatic flexible active skin based on a shape memory polymer (SMP). Each actuator has a diameter of 3 mm, and is placed on a 4-mm pitch. The device was demonstrated as active camouflage and tactile display with a stroke

of 0.4 mm. The pitch and the stroke do not match the requirements for Braille text which are typically 2.5 mm and 0.5-0.6 mm respectively.

Here, we report a high resolution pneumatic tactile display that can exert large stroke and provide high blocking force. The device exploits the large stiffness change of the BSEP polymer and large-strain deformation of the polymer at the softened state. A serpentine-patterned carbon nanotube coating composited on the BSEP membrane surface is used to administer local temperature change and the membrane's stiffness. A single pneumatic reservoir is employed to deform all the softened areas at once. The tactile display can be actuated at low voltage supply (30 V) to obtain large stroke, high blocking force, and safe operation with fast response speed. Potential applications for such a tactile display are numerous, such as reproducing surface topography, providing haptic feedback for human-machine interfaces, and electronic Braille readers.

2. EXPERIMENTAL SECTION

2.1. Materials. Urethane diacrylate (UDA, catalog name: CN9021) was obtained from SARTOMER and used as received. Stearyl acrylate (SA), trimethylolpropane triacrylate (TMPTA), acrylic acid (AA), 2,2-Dimethoxy-2-phenylacetophenone (DMPA), benzophenone (BP), and isopropyl alcohol (IPA) were purchased from Sigma-Aldrich and used as received. Single-walled carbon nanotubes (catalog name: P3-SWNT) were purchased from Carbon Solutions, Inc.

2.2. BS80-AA5 Thin Film Fabrication. The prepolymer solution was made by mixing 80 parts (by weight) of SA, 20 pats of UDA, 5 parts of AA, 1.5 parts of TMPTA, 0.25 part of DMPA, and 0.125 part of BP at 50 ^{o}C. The prepolymer solution was then injected between a pair of glass slides on a hot plate with two strips of tape as spacers. The thickness of the liquid layer was defined by

the thickness of the spacers. In the device assembling, 90 μm thick spacers were used to fabricate the BSEP film. Next, the prepolymer was cured through a UV curing conveyor equipped with a Fusion 300S type "H" UV curing bulb for about 3min. Then the film can be gently peeled off the glass slide after it cooled down to room temperature.

2.3. Serpentine Patterned Carbon Nanotube (S-CNT) Joule Heating Electrode Fabrication. The carbon naotube (CNT) dispersion solution was made by mixing 5 mg of P3-SWNT powder, 1 ml water, and 20 ml IPA. The mixture was bath sonicated for 90 min to get a stable dispersion. Large aggregates were disposed using centrifuge at 8500 rpm for 10 min. The resulting supernatant is then ready for spray coating.

The stretchable S-CNT electrode was obtained by first prestretching the softened BSEP film by 100% × 100% biaxially. The prestretched film was then cooled down to room temperature to preserve the deformation. Next, a shadow mask with serpentine pattern cutout was attached to the prestretched rigid BSEP. The prepared CNT dispersion solution was sprayed on BSEP through the mask using an airbrush at an air pressure of 30 psi. Next, a solution of UDA in toluene (10 vol%) was sprayed and cured on top of the entire film without the mask. The thickness of the poly(UDA) layer is around 5 μm. Finally, the film recovered to its original size by heating and releasing the prestretch.

2.4. Device Assembling. The resulting film of BSEP with S-CNT was attached to the chamber cover (17 mm × 17 mm) with a double-sided Kapton™ tape as adhesive layer in between. The double-sided tape was cut with openings that align with the S-CNT matrix. The whole device could be assembled by screwing the chamber cover with the pneumatic chamber.

3. RESULTS AND DISCUSSION

3.1. Device Design and Fabrication. The demonstrated tactile device contains a 4 by 4 tactile pixel (taxel) matrix with outer size of 17 mm × 17 mm × 3 mm (Figure 1a). Each taxel has 1.5 mm diameter with 2.5 mm distance between the centers of two adjacent taxels (designed according to Braille standard[28]). The device primarily consists of two parts: a pneumatic system and a thin BSEP active film that can be thermally controlled to soften locally. The pneumatic system constitutes a pneumatic chamber and a miniature pump to provide pressurized air for actuation. The specific BSEP polymer used is a phase changing polymer that exhibits stiffness change of three orders of magnitude in a narrow temperature range of less than 10 ºC [29]. At room temperature, the BSEP possesses a modulus of several hundred MPa, and behaves as a rigid plastic, capable of providing a blocking force as high as 50 g. Above its transition temperature, the polymer becomes soft and stretchable with its modulus decreasing to 0.1 MPa. The BSEP active film has a thickness of about 90 μm. A matrix of highly compliant single-walled CNT Joule heating electrode patterned in serpentine shape (S-CNT) is formed on the surface of the BSEP film. The thermal stability, mechanical compliancy, and chemical resistance of CNTs made it an ideal choice as the Joule heating electrode [30,31]. The BSEP with S-CNT electrode is attached on the chamber to make the chamber relatively air-tight. The rigid chamber cover is then mounted using an adhesive tape and 4 corner screws. The circular openings on the adhesive tape and the chamber cover aligns with the S-CNT electrode areas, each defining a taxel area. A pin with a flange on one end to prevent it from dropping out of the taxel cell is placed in each taxel. The protruding surface of the pin is the tactile interface of the taxel. As each taxel has an independent S-CNT Joule heating electrode, the modulus of the BSEP can be altered locally, enabling individual taxel control of the display panel. By synchronizing the pneumatic pressure and thermal stimuli, the BSEP can be locally softened and deformed, thereby raising individual pins by 0.7 mm in height (Figure S1) and presenting

unique configurations to the end user. Upon cooling, the BSEP rigidifies, which takes less than 2 s, no external energy input is then needed. In figure 1C, the 4 × 4 tactile display shows "U" "C" "L" "A" on the device, demonstrating the precise control of individual dots. The display can be quickly refreshed by reheating the deformed taxels without applying any pneumatic pressure.

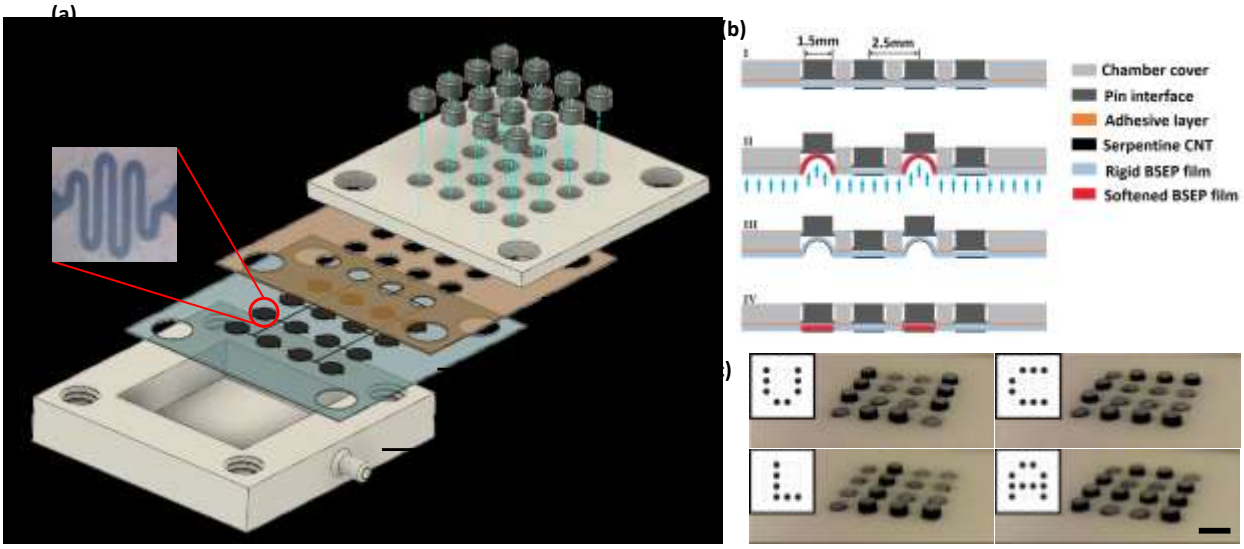

Figure 1. A compact tactile display. (**a**) Schematic of the layered structure of a 4 ×4-pixel array. (**b**) Cross sectional view of the working mechanism. The taxels, with Braille size (I), is individually actuated by softening (50 ºC) and deforming the BSEP in corresponding area (II). The deformation is then maintained without any energy input when the BSEP film cools below 40 ºC (III). The original shape is recovered by reheating the BSEP (IV). (**c**) Demonstration of a 4x4 tactile display showing "U", "C", "L", "A". The scale bar represents 2 mm.

The core component in the pneumatic tactile display is the BSEP film with stretchable Joule heating electrode. To obtain high stretchability, we developed a "P3R" fabrication process: Prestretch-Pattern-Protect-Release (Figure 2a). The method starts with prestretching a softened BSEP film biaxialy by 100% × 100%. The prestretched film maintains the stable deformed-shape after it cools down. A dispersion solution of CNTs in an isopropyl alcohol and water mixture solvent is then sprayed on the prestretched BSEP through a shadow mask. The mask has a serpentine shaped cutout pattern formed by laser ablation. Next, a solution of urethane diacrylate (UDA) monomer in toluene is sprayed on top of the CNT-coated BSEP film. Because of its low viscosity, the UDA solution infiltrates into the CNT network, forming an ultra-thin CNT-poly(UDA) interpenetrating composite electrode after the UDA layer is cured. As the CNT network is embedded into the poly(UDA) layer, physical translation of CNTs is largely prevented during the deformation of the BSEP film. Moreover, since the UDA monomer is also one of the co-monomers to form the BSEP, the poly(UDA) layer strongly bonds the BSEP film. When the resulting poly(UDA)/CNT/BSEP composite structure is heated above the BSEP's melting temperature (T_m) to release the prestretch in the BSEP layer, the BSEP matrix along with the S-CNT electrode shrinks 100% × 100% biaxially, while the poly(UDA) layer wrinkles up (Figure 2b). The wrinkled topography is shown as a "greasy" surface in the upper microscopic image, whereas the flat surface of the CNT/BSEP electrode prepared without the poly(UDA) shows a "dry" surface. Note that the "greasy" surface is resulted from the surface unevenness that blurs the optical image and imparts the S-CNT electrode with high stretchability. This P3R method and the serpentine shaped pattern of the CNT layer afford an active BSEP film with a highly compliant and stretchable Joule heating electrode.

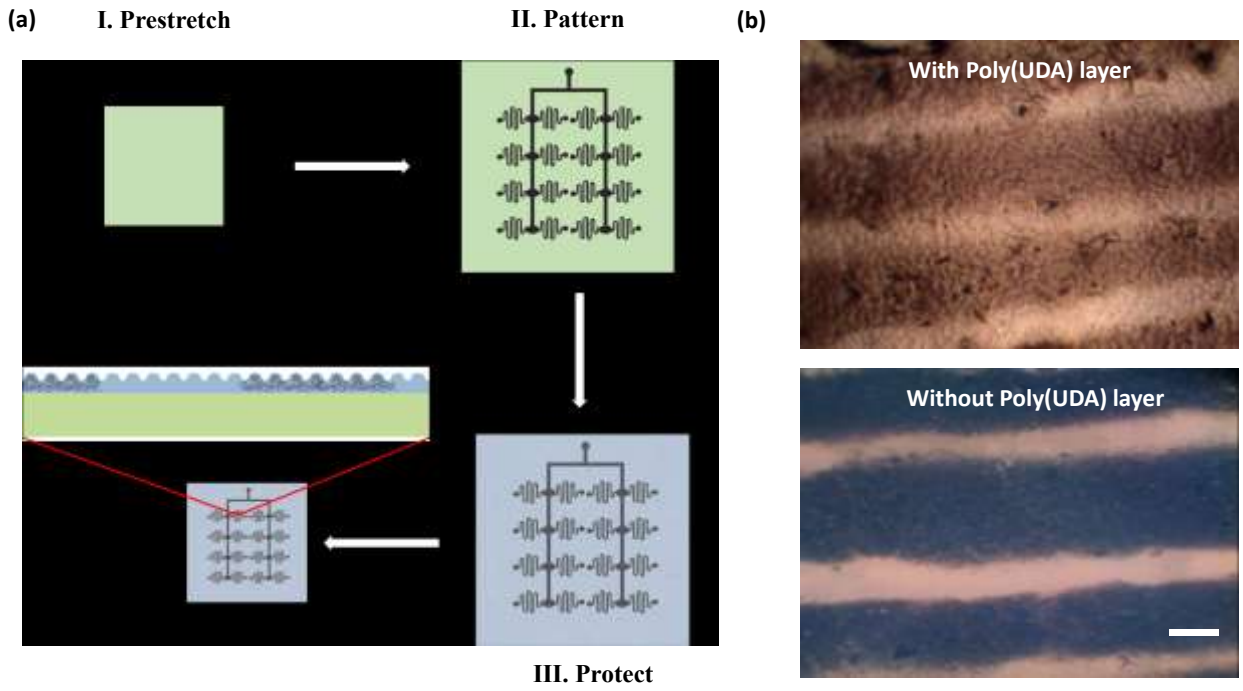

Figure 2. (a) Schematic illustration of the "P3R" fabrication process of BSEP film with serpentine CNT Joule heating electrode. (I) Prestretch: the BSEP film is prestretched biaxially at elevated temperature and then cooled down. (II) Pattern: a carbon nanotube solution is spray coated on the prestretched BSEP through a shadow mask. (III) Protect: A monomer (UDA) solution is spray-coated on the CNT electrode and cured, forming a CNT-poly(UDA) interpenetrating composite. (IV) Release: the prestrain is released by softening the BSEP film. (b) Optical microscopic images of the BSEP active layer with (above) and without (bottom) the poly(UDA) layer. The scale bar represents 0.1 mm.

3.2. Bistable Electroactive Polymer (BSEP). Variable stiffness material has been an actively researched subject for decades because the ability of muscle to adjust its modulus is responsible for the adaptability and dexterity of animals. Shape memory polymers (SMP), which exhibit a modulus change by a few hundred-fold during glass transition [32,33], can be programed to different rigid shapes via stretching at elevated temperatures[34]. Glass transition typically spans in a broad temperature range of over 20 ^{o}C[24] which limit the utility of these materials. For applications involving human tactile interaction[27], the SMP needs to remain rigid up to around 37 ^{o}C to prevent incidental shape changes. The actuation would be conducted above the polymer's glass transition temperature (T_g), or more than 20 ^{o}C above body temperature which could induce tissue damage. This limitation is addressed in this work with a phase changing BSEP polymer we recently developed comprising stearyl acrylate (SA) moiety in the polymer that can reversibly crystallize and melt within a narrow temperature range [29] (Figure S2). The phase change occurs within 10 ^{o}C and induces a modulus change of nearly 1000-fold.

The compounds used to synthesize the phase changing BSEP are shown in Figure S3, and the synthetic details are found in the experimental section. To obtain the optimal overall performance for tactile display application, the BSEP was formulated to contain 80 parts of SA (by weight), 20 parts of UDA, 5 parts of acrylic acid (AA), 1.5 parts of TMPTA, 0.25 part of DMPA, and 0.125 part of BP, and the polymer is labeled as BS80-AA5. Adding the small amount of acrylic acid was found to help increase the modulus change, mechanical toughness, and electrode bonding.

Stiffness change is critical for BS80-AA5 to maintain the actuated shape. The hydrogen bonds from the carboxylic acid group in AA helped increase the difference in modulus between room temperature and elevated temperature. At room temperature, the carboxylic acid groups form double hydrogen bonding dimers which help further increase the stiffness.[35] With increasing

temperature, the hydrogen bonds weaken, thus have diminished effect on the modulus of the softened BSEP. Dynamic mechanical analysis of the BSEP polymer was conducted at a temperature ramping rate of 2 ºC/min from 25 to 55 ºC and a mechanical loading frequency of 1 Hz. Figure 3a shows that BS80-AA5 possesses a steep stiffness change of 3000 times from about 300 MPa to about 0.1 MPa. The transition occurs from 40 ºC to 47 ºC. Once the transition is completed, the storage modulus remains constant with further increasing temperature. The ultralow modulus of only 0.1 MPa in the rubbery state is resulted from the presence of large amount of molten stearyl chains which serve as plasticizers to the polymer. The substantial modulus switching leads to high shape memory property (Figure S4). In fact, the fixation rate and recovery rate of BS80-AA5 are both close to 100%.

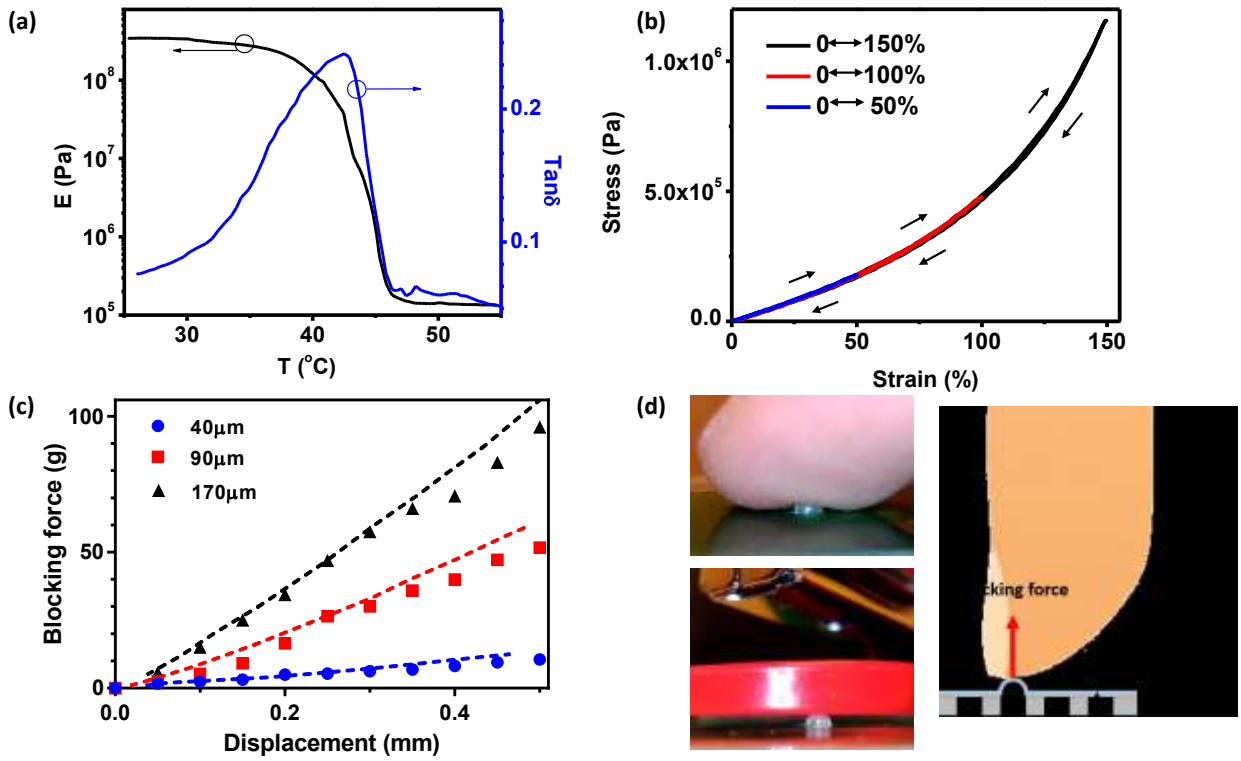

Figure 3. Mechanical properties of BS80-AA5. (a) The sharp change of storage modulus and loss factor with respect to temperature. (b) Cyclic tensile loading-unloading tests of BS80-AA5 under different stretch ratio with strain rate of 0.01 /s. (c) Measured (symbols) and simulated (dashed curves) blocking force required to completely press down an actuated BS80-AA5 taxel with different displacement. The thickness of the un-deformed BSEP films ranges from 40 μm to 170 μm. (d) Pictures showing a rigid BSEP taxel with 90 μm thick BSEP capable of deforming a user's fingertip (up left) and supporting a 25 g mini stapler (down left), and a schematic illustration of measured blocking force (right).

An essential requirement for the refreshable tactile display is the reversibility and repeatability of the taxel actuation over many cycles. The elasticity of BS80-AA5 in the rubbery state was thus characterized. The loss factor of the softened BS80-AA5 is around 0.05 (Figure 3a), which indicates very low viscoelasticity and thus fast response speed. Cyclic tensile tests were also carried out at 50 ºC with a strain rate of 0.01 s^{-1}. The tests consisted of three loading-unloading loops with strain successively up to 50%, 100%, and 150%, respectively, in three separate tests. The resulting stress-strain curves are shown in Figure 3b where the loading and unloading curves completely overlap, suggesting that the material behaves elastically with minimal hysteresis, thereby agreeing with the low loss factor measured in dynamic mechanical analysis. Another important requirement for BS80-AA5 to resist fracture during stretching is high toughness. The hydrogen bonds from acrylic acid act as reversible crosslinks to enhance the toughness. Physical crosslinks have been identified as an essential element to toughen soft gels.[36–38] The non-permanent crosslinks can break and re-form to overcome stress concentration and dramatically enhance crack propagation resistance. The comparison of toughness between BS80-AA5 and BS80 (without acrylic acid) was characterized via uniaxial tensile test at 50 ºC (Figure S5). The BS80-AA5 has a maximum elongation of 320% with a normal tensile strength of 8 MPa and true tensile strength calculated to be 34 MPa. Without the toughening effect from acrylic acid, BS80 ruptured at 191% strain with a tensile strength of only 0.26 MPa (true stress calculated to be 0.76 MPa). Moreover, the highly stretchable poly(UDA) layer helped further increase the maximum elongation and tensile strength of BS80-AA5/poly(UDA) film without having much impact on the storage modulus of the composite film (Figure S6). The high tensile strength of BS80-AA5 is important for the polymer to resist against fracture. Meanwhile, the stress to obtain up to 200% strain is low, i.e., the softened BS80-AA5 is highly compliant, and large deformation could be

obtained with low pneumatic pressure. The air pressure needed to actuate a taxel to different heights was measured and the results are shown in Figure S7. For a 90 μm thick BSEP film, the pressure to generate an out-of-plain displacement of 0.7 mm (minimum displacement requirement for Braille is 0.5 mm[28]) is only 160 mmHg.

In the rigid state of the BSEP polymer, the crystalline aggregates of the SA moieties act as hard segments in the polymer, resulting in a storage modulus of 340 MPa. The taxels are thus expected to be able to resist large forces applied to the raised dots. The blocking force, or force required to press down the raised dots to completely overcome the original vertical displacement, was measured for taxels in which the BSEP polymer had originally been actuated into various raised height. Note that raised height of 0.75 mm means the BSEP film was actuated to a half-dome shape with an area expansion of 100%. The results are shown in Figure 3c for BS80-AA5 films with undeformed thickness ranging from 40 μm to 170 μm. ANSYS Finite Element Analysis (FEA) was also performed to simulate the blocking force of the taxels based on Yeoh's 3rd hyperelastic model. The FEA simulation results match the experimental data quite well. More information about FEA simulations can be found in supporting information. For the tactile display panel we fabricated, the BSEP film with un-deformed thickness of 90 μm was used. The rigid taxels with actuated displacement of 0.5 mm have a blocking force of 50 g, which is much greater than the 15 g requirement in typical tactile devices[28]. Supplementary Video shows an actuated taxel dot capable of supporting vigorous tapping and rubbing from a user's finger without deforming, suggesting that the rigid BSEP actuator is strong enough for repeating heavy touches.

3.3. Serpentine CNT Joule Heating Electrode. Mechanical impedance of the Joule heating electrode coated on the BSEP film can alter the actuated strain (raised height) and uniformity (shape of the raised dome structure). It is essential to develop a heating electrode that is both highly

compliant and stretchable. In recent years, great efforts have been made to develop stretchable conductors for the next generation of flexible and wearable electronics that can conform to movable and arbitrarily shaped surfaces[39–41]. However, much of these reported stretchable conductors are too stiff for the present application. We selected carbon nanotube as the Joule heating electrode material thanks to the nanotubes' large length-to-diameter aspect ratio that form highly porous percolation networks and have high thermal and environmental stability. The Joule heating requires a thick coating of CNT to obtain low surface resistance for low-voltage heating, but a thick coating would induce significant mechanical impedance[30] and may delaminate from the polymer matrix. Moreover, with such high resolution, where the closest distance between two adjacent taxels is only 1 mm, it is essential for the Joule heating electrodes to obtain uniform and precise heating to prevent crosstalk. To overcome these issues, the "P3R" fabrication process: Prestretch-Pattern-Protect-Release was employed to obtain simultaneously low surface resistance, low mechanical impedance, and high stretchability.

The carbon nanotubes (P3-SWNT, Carbon Solutions, Inc) we used for the electrode were specifically tailored for dispersion in solvents, and contain 6% carboxylic acid groups (SWNT-COOH) [42]. The SWNT-COOH bonds to BS80-AA5 strongly through the hydrogen bonding interactions between the carboxylic acid groups[35]. Figure S8 demonstrates the CNT electrode on a BS80-AA5 film capable of surviving multiple tape peeling tests. A Kapton™ tape with a high peeling strength of 46 oz/in was used to check if the CNT could be removed during peeling. After several peeling processes, the resistance and the color of the CNT electrode on BS80-AA5 didn't change at all, suggesting strong bonding between CNT and BS80-AA5. In comparison, the CNT electrode similarly formed on a BS80 film were almost completely transferred to the tape after one test, and lost surface conductivity.

The heating process is the most critical step in the operation of the tactile display device. To achieve high-efficiency heating with low mechanical impedance, we fabricated the CNTs into a serpentine shape. The serpentine architecture has been explored by a number of research groups as an effective approach to impart large stretchability to electrodes.[43–47] As Joule heating electrode, a more important character is uniform and rapid heating. With applied voltage, the charge carriers will be restricted within the winding path of the serpentine pattern, resulting in uniform heating over the taxel area (Figure S9a and S9c). On the other hand, for the conventionally-used round-shaped pattern, the charge carriers tend to travel the shortest distance, causing the current density to mainly distribute along the equatorial area (Figure S9b and S9d). In our device, the resistance of one S-CNT was kept at around 40-50 kΩ to ensure low voltage (~ 30 V) activation for the device. As shown in Figure S9e, the time needed for the serpentine shaped electrode to reach 47 ºC, which is the temperature to soften BS80-AA5, is less than 1 s, while it takes more than 5 s for the round shaped electrode (with same resistance) to reach 40 ºC. The unique winding path of the S-CNT increases the heating efficiency, resulting in rapid and uniform heating in a very short time. The short heating duration also prevents excessive heat dissipation which not only consumes more electrical energy, but also could cause thermal crosstalk with neighboring pixels. Moreover, the serpentine pattern is also very effective to retain the compliancy of the Joule heating electrode. Under the same electrode loading per unit area, the storage moduli of the poly(UDA)/CNT/BS80-AA5 films where the CNT electrode is either blanket-coated or serpentine-patterned are 1.9 MPa and 0.36 MPa, respectively, at 50 ºC. Both moduli are higher than that of the softened BS80-AA5 film which is 0.13 MPa at 50 ºC. Note that PUDA layer has higher stiffness compare to BS80-AA5, which also contributes in the modulus increase (Figure S6b). High compliancy of the S-CNT electrode is essential for the low air-pressure actuation.

Joule heating characteristics of the S-CNT electrode under different voltages were also investigated, and the results are shown in Figure S10. The electrode exhibits high heating rate, considering the high resistance of the S-CNT electrode. Complete softening (above 47 ^{o}C) could be obtained in less than 1 second at 30 V operation. The cooling process to below 40 ^{o}C to stiffen BS80-AA5 requires about 2 seconds. The air flow in the diaphragm configuration induced by the pneumatic pumping could facilitate heat dissipation to further driving down the duration of the cooling step. Thus, a taxel actuation cycle can be completed in 3 seconds. The thermal and pneumatic control sequence of the taxel actuation is illustrated in Figure S11. After one second, the Joule heating can be turned off, while the pneumatic pump is turned on. Because of the elastic nature of the BS80-AA5 film, once the pump is on, the pin interface is lifted immediately. Then the pump can be turned off in 2 seconds when the film has cooled down.

To ensure stable heating during actuation, the resistance of the Joule heating electrode needs to remain constant. In our device, to latch a 0.7 mm displacement, the BSEP active layer needs to expand about 100% area strain to form a half spherical dome. In other words, the Joule heating electrode needs to be compliant enough to be stretched by 100% area strain without much restriction to the polymer matrix, while maintaining a constant resistance to allow for consistent heating steps. Figure 4a shows the normalized resistance of a braille sized S-CNT electrode on BS80-AA5 in response to area expansion on a diaphragm. The resistance stays almost constant with area strain up to about 200% and increases dramatically with further increase strain. Such behavior is reasonable because of the “Prestretch-Release” steps in the P3R fabrication process mentioned above. In the “Prestretch” step, the BSEP film is prestretched to about 100% $\times$ 100% biaxial strain (300% area strain). The following “Releasing” step causes the CNT coating embedded in the P(UDA) layer to wrinkle with the P(UDA) layer. Subsequent stretching translates

into flattening of the wrinkles without substantial elongation within the CNT coating and thus ensures a relatively constant resistance until the wrinkles has been flattened and further stretching leads to elongation within the S-CNT coating. To obtain high stretchability and durability of the S-CNT electrode, interpenetration of the CNT network within the protecting P(UDA) layer is important to prevent the carbon nanotubes from translational movement during repetitive deforming-recovering cycles.

Cyclic stretching test was also carried out on one taxel. Under induced area strain of 100%, which will exert a displacement over 0.7 mm, the resistance and Joule heating characteristics remain stable for over 100,000 repetitive cycles at a frequency of 0.8 Hz (Figure 4b). The upper insets show optical microscope images of a continuous electrode line of the S-CNT electrode before and after the 100,000 cycles of lifetime test. Uniform and precise heating was observed from the infrared thermal images of the electrode before and after the test (lower insets). Figure 4c compares heating rate, stretchability, and resistance consistency of S-CNT electrode with other reported compliant and stretchable Joule heating films that can generate uniform heat across the surface. The main efforts of contemporary research activities on stretchable heaters are focused on low dimensional carbon materials (filled symbols)[48–51], metal nanowires: silver based (open symbols) [52–56] and copper based (half-filled symbols)[57–60], and conductive polymers (half-filled pentagon)[61]. The S-CNT electrode can simultaneously perform fast heating rate (31 ^{o}C/s), large stretchability (188% area strain), and high resistance consistency (98.9% resistance recovery after one cycle), which can be very challenging for most other reported Joule heating electrodes to fulfill all three-performance metrics at the same time. Figure 4d demonstrates a Braille cell device using the S-CNT-BSEP system, which shows “U” “C” “L” “A” in Braille characters. The insets are the

corresponding infrared images of working S-CNT Joule heating electrodes. The heating is precise and uniform without any crosstalk between adjacent dots.

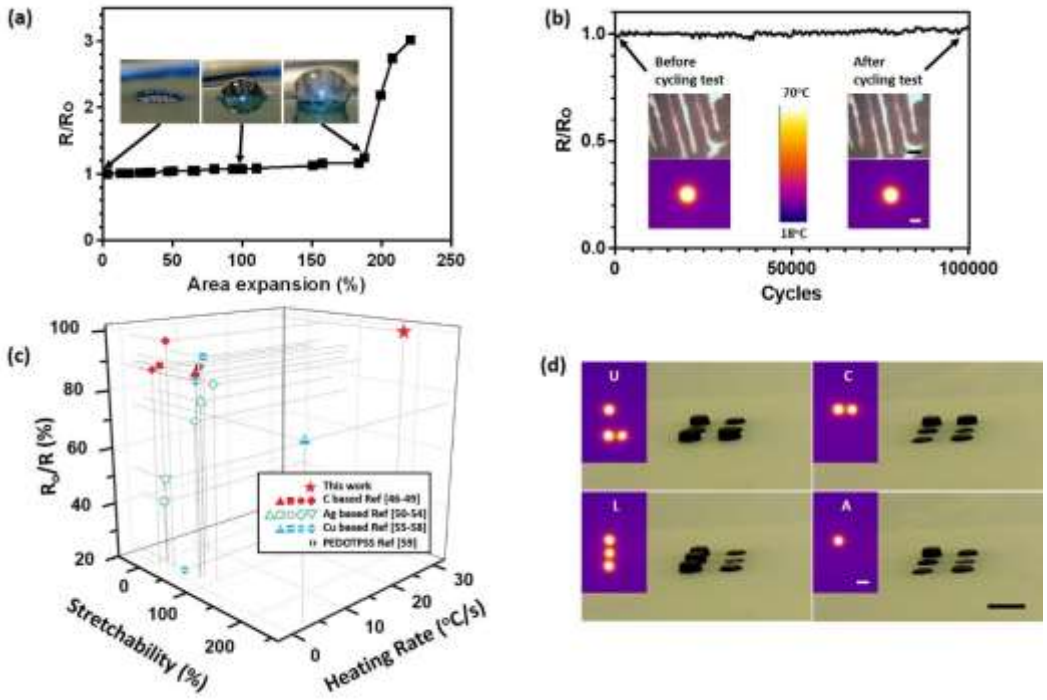

Figure 4. Performance of S-CNT Joule heating electrode. (a) Relative resistance variation of a serpentine CNT electrode under different area expansion. (b) Lifetime test on a serpentine CNT Joule heating electrode with 100% area expansion deforming and releasing cycle at a frequency of 0.8 Hz for over 100,000 cycles. The insets show the serpentine CNT electrode retaining the continuous electrode line (up left and up right, scale bar 0.2 mm) and stable heating (down left and down right, scale bar 1 mm) after the cycling test. (c) Comparison of heating performance of important stretchable Joule heating films with respect to heating rate, stretchability, and resistance consistency. Heating rates of the literature films were calculated from reported temperature versus time curve under the highest voltage provided. If not specified in the literature, stretchability was defined as the stretch ratio when the resistance increases by 20%. The resistance consistency was

obtained by initial resistance over the resistance after a stretch-release cycle. (d) Demonstration of a one-cell Braille device showing “U” “C” “L” “A” in Braille characters with infrared images of the corresponding S-CNT Joule heating electrode shown to the left. The scale bars are 2 mm.

High energy consumption is often cited as the key drawback for using shape memory polymers and alloys for shape change. For the proposed tactile display, the Joule heating electrode is patterned directly and only on the active taxel areas. The area being heated is only 1.77 mm^2 per taxel pixel, and the polymer film is 90 μm thickness. In a typical experiment, 30 V was applied to the serpentine CNT electrode of 50 kΩ resistance, it took 1 second to reach 50 ^oC. The power consumption is calculated to be 18 mW. For a smartphone screen sized panel with 48 × 24 taxels, roughly 50% of the dots are raised during content refreshing, so the total power consumption is 2.16 W. The switching circuit and the pneumatic pump also consume about 1 W during operation. The overall power consumption is thus 3.16 W which is within the useful range for small or portable devices. In comparison, the peak power consumption of iPhone X® is 10.5 W. The power supply required for the Hyperbraille S Display 6240 from Metec® is 48 W.

4. CONCLUSIONS

A refreshable tactile display with Braille standard resolution has been demonstrated. The steep modulus change of BS80-AA5 over a narrow temperature range grants the device with high blocking force of over 50 g and large displacement of 0.7 mm. The “P3R” fabrication process of Prestretch-Pattern-Protect-Release is effective to form a S-CNT electrode in the wrinkled surface layer with high compliancy and resistance-consistence up to 188% area strain. The electrode can soften the BSEP film at 30 V in less than 1 s. The simple architecture of the tactile display ensures an easy and low-cost fabrication. The demonstrated refreshable tactile display should find a wide

range of applications in rehabilitation of people with vision impairment, entertainment, robotics, health care, and so on.

ASSOCIATED CONTENT

Supporting Information

Finite element analysis simulation; demonstration of 4 × 4 tactile display actuation; bistable mechanism of BSEP material; chemical structures of monomers and initiators of BS80-AA5; shape memory demonstration of BS80-AA5; tensile test measurements comparison between BS80-AA5 and BS80; mechanical property measurements of poly(UDA), BS80-AA5, and BS80-AA5/poly(UDA); actuation height of BSEP films under different pneumatic pressure activations; electrode-substrate bonding test; Joule heating behavior between serpentine-shaped and round-shaped electrode; Joule heating characterization of S-CNT under different voltages; thermal and pneumatic control sequence (PDF)

Actuation demonstration of one tactile dot (AVI)

AUTHOR INFORMATION

Corresponding Author

*E-mail: qpei@seas.ucla.edu (Q.P.).

ORCID

Yu Qiu: 0000-0002-2707-3993

Zhiyun Lu:

Qibing Pei: 0000-0003-1669-1734

Author Contributions

The manuscript was written through contributions of all authors. All authors have given approval to the final version of the manuscript.

Funding Sources

The work was supported by National Science Foundation (award number 1700829 and award number 1638163).

Notes

The authors declare no competing financial interest.

ACKNOWLEDGMENT

The work was supported by the National Science Foundation (award number 1700829 and award number 1638163). The authors thank Dr. Rujun Ma and Dr. Yuan Meng for valuable discussions.

ABBREVIATIONS

BSEP, bistable electroactive polymer; UDA, urethane diacrylate; P3R, Prestretch-Pattern-Protect-Release; S-CNT, serpentine-carbon nanotube.

REFERENCES

(1) Dang, T.; Annaswamy, T. M.; Srinivasan, M. A. Development and Evaluation of an Epidural Injection Simulator with Force Feedback for Medical Training. *Stud. Health Technol. Inform.* **2001**, *81* (August), 97–102.

(2) Langrana, N. A.; Burdea, G.; Lange, K.; Gomez, D.; Deshpande, S. Dynamic Force Feedback in a Virtual Knee Palpation. *Artif. Intell. Med.* **1994**, *6* (4), 321–333.

(3) Vining, D. J.; Liu, K.; Choplin, R. H.; Haponik, E. F. Virtual Bronchoscopy: Relationships of Virtual Reality Endobronchial Simulations to Actual Bronchoscopic Findings. *Chest* **1996**, *109* (2), 549–553.

(4) Maisto, M.; Pacchierotti, C.; Chinello, F.; Salvietti, G.; De Luca, A.; Prattichizzo, D. Evaluation of Wearable Haptic Systems for the Fingers in Augmented Reality Applications. *IEEE Trans. Haptics* **2017**, *10* (4), 1–1.

(5) Bouzit, M.; Burdea, G.; Popescu, G.; Boian, R. The Rutgers Master II - New Design Force-Feedback Glove. *IEEE/ASME Trans. Mechatronics* **2002**, *7* (2), 256–263.

(6) Cortesao, R.; Park, J.; Khatib, O. Real-Time Adaptive Control for Haptic Manipulation with Active Observers. *Proc. 2003 IEEE/RSJ Int. Conf. Intell. Robot. Syst. (IROS 2003) (Cat. No.03CH37453)* **2003**, *3* (October), 2938–2943.

(7) Turner, M. L.; Gomez, D. H.; Tremblay, M. R.; Cutkosky, M. R.; Alto, P. Preliminary Tests of an Arm-Grounded Haptic Feedback Device in Telemanipulation. *Proc. ASME IMECE Haptics Symp.* **1998**, 1–6.

(8) Choi, H. R.; Lee, S. W.; Jung, K. M.; Koo, J. C.; Lee, S. I.; Choi, H. G.; Jeon, J. W.; Nam, J. D. Tactile Display as a Braille Display for the Visually Disabled. *2004 IEEE/RSJ Int. Conf. Intell. Robot. Syst. (IEEE Cat. No.04CH37566)* **2004**, *2*, 1985–1990.

(9) King, H. H.; Donlin, R.; Hannaford, B. Perceptual Thresholds for Single vs. Multi-Finger Haptic Interaction. *2010 IEEE Haptics Symp. HAPTICS 2010* **2010**, 95–99.

(10) Motto Ros, P.; Dante, V.; Mesin, L.; Petetti, E.; Del Giudice, P.; Pasero, E. A New Dynamic Tactile Display for Reconfigurable Braille: Implementation and Tests. *Front. Neuroeng.* **2014**, *7* (April), 6.

(11) Summers, I. R.; Chanter, C. M. A Broadband Tactile Array on the Fingertip. *J. Acoust. Soc. Am.*

2002, *112* (August), 2118–2126.

(12) Wagner, C. .; Lederman, S. J.; Howe, R. D. Design and Performance of a Tactile Shape Display. *Haptics-e* **2004**, 6.

(13) Velazquez, R.; Pissaloux, E. E.; Hafez, M.; Szewczyk, J. Tactile Rendering with Shape-Memory-Alloy Pin-Matrix. *IEEE Trans. Instrum. Meas.* **2008**, *57* (5), 1051–1057.

(14) Lee, J. S.; Lucyszyn, S. A Micromachined Refreshable Braille Cell. *J. Microelectromechanical Syst.* **2005**, *14* (4), 673–682.

(15) Kwon, H. J.; Lee, S. W.; Lee, S. S. Braille Dot Display Module with a PDMS Membrane Driven by a Thermopneumatic Actuator. *Sensors Actuators, A Phys.* **2009**, *154* (2), 238–246.

(16) Vidal-Verdú, F.; Madueño, M. J.; Navas, R. Thermopneumatic Actuator for Tactile Displays and Smart Actuation Circuitry. *Proc. SPIE - Int. Soc. Opt. Eng.* **2005**, *5836* (July 2005), 484–492.

(17) Koo, I. M.; Jung, K.; Koo, J. C.; Nam, J. Do; Lee, Y. K.; Choi, H. R. Development of Soft-Actuator-Based Wearable Tactile Display. *IEEE Trans. Robot.* **2008**, *24* (3), 549–558.

(18) Matysek, M.; Lotz, P.; Winterstein, T.; Schlaak, H. F. Dielectric Elastomer Actuators for Tactile Displays. *Proc. - 3rd Jt. EuroHaptics Conf. Symp. Haptic Interfaces Virtual Environ. Teleoperator Syst. World Haptics 2009* **2009**, 290–295.

(19) Jungmann, M.; Schlaak, H. F. Miniaturised Electrostatic Tactile Display with High Structural Compliance. *Proc. Conf. Eurohaptics* **2002**, No. August, 12–17.

(20) De Rossi, D.; Carpi, F.; Carbonaro, N.; Tognetti, A.; Scilingo, E. P. Electroactive Polymer Patches for Wearable Haptic Interfaces. *Proc. Annu. Int. Conf. IEEE Eng. Med. Biol. Soc. EMBS* **2011**, No. Section III, 8369–8372.

(21) Lee, H. S.; Phung, H.; Lee, D. H.; Kim, U. K.; Nguyen, C. T.; Moon, H.; Koo, J. C.; Nam, J. Do;

Choi, H. R. Design Analysis and Fabrication of Arrayed Tactile Display Based on Dielectric Elastomer Actuator. *Sensors Actuators, A Phys.* **2014**, *205*, 191–198.

(22) Phung, H.; Nguyen, C. T.; Nguyen, T. D.; Lee, C.; Kim, U.; Lee, D.; Nam, J. Do; Moon, H.; Koo, J. C.; Choi, H. R. Tactile Display with Rigid Coupling Based on Soft Actuator. *Meccanica* **2015**, *50* (11), 2825–2837.

(23) Chakraborti, P.; Toprakci, H. A. K.; Yang, P.; Di Spigna, N.; Franzon, P.; Ghosh, T. A Compact Dielectric Elastomer Tubular Actuator for Refreshable Braille Displays. *Sensors Actuators, A Phys.* **2012**, *179* (June), 151–157.

(24) Yu, Z.; Yuan, W.; Brochu, P.; Chen, B.; Liu, Z.; Pei, Q. Large-Strain, Rigid-to-Rigid Deformation of Bistable Electroactive Polymers. *Appl. Phys. Lett.* **2009**, *95* (19), 21–24.

(25) Wu, X.; Kim, S. H.; Zhu, H.; Ji, C. H.; Allen, M. G. A Refreshable Braille Cell Based on Pneumatic Microbubble Actuators. *J. Microelectromechanical Syst.* **2012**, *21* (4), 908–916.

(26) Yobas, L.; Huff, M. A.; Lisy, F. J.; Durand, D. M. A Novel Bulk-Micromachined Electrostatic Microvalve with a Curved-Compliant Structure Applicable for a Pneumatic Tactile Display. *J. Microelectromechanical Syst.* **2001**, *10* (2), 187–196.

(27) Besse, N.; Rosset, S.; Zarate, J. J.; Shea, H. Flexible Active Skin: Large Reconfigurable Arrays of Individually Addressed Shape Memory Polymer Actuators. *Adv. Mater. Technol.* **2017**, *1700102*, 1700102.

(28) Runyan, N. H.; Carpi, F. Seeking the `holy Braille' Display: Might Electromechanically Active Polymers Be the Solution? *Expert Rev. Med. Devices* **2011**, *8* (5), 529–532.

(29) Ren, Z.; Hu, W.; Liu, C.; Li, S.; Niu, X.; Pei, Q. Phase-Changing Bistable Electroactive Polymer Exhibiting Sharp Rigid-to-Rubbery Transition. *Macromolecules* **2016**, *49* (1), 134–140.

(30) Yuan, W.; Hu, L.; Yu, Z.; Lam, T.; Biggs, J.; Ha, S. M.; Xi, D.; Chen, B.; Senesky, M. K.; Grüner, G.; Pei, Q. Fault-Tolerant Dielectric Elastomer Actuators Using Single-Walled Carbon Nanotube Electrodes. *Adv. Mater.* **2008**, *20* (3), 621–625.

(31) Yamada, T.; Hayamizu, Y.; Yamamoto, Y.; Yomogida, Y.; Izadi-Najafabadi, A.; Futaba, D. N.; Hata, K. A Stretchable Carbon Nanotube Strain Sensor for Human-Motion Detection. *Nat. Nanotechnol.* **2011**, *6* (5), 296–301.

(32) Niu, X.; Yang, X.; Brochu, P.; Stoyanov, H.; Yun, S.; Yu, Z.; Pei, Q. Bistable Large-Strain Actuation of Interpenetrating Polymer Networks. *Adv. Mater.* **2012**, *24* (48), 6513–6519.

(33) Meng, Y.; Jiang, J.; Anthamatten, M. Body Temperature Triggered Shape-Memory Polymers with High Elastic Energy Storage Capacity. *J. Polym. Sci. Part B Polym. Phys.* **2016**, *54* (14), 1397–1404.

(34) Hu, X.; Zhou, J.; Vatankhah-Varnosfaderani, M.; Daniel, W. F. M.; Li, Q.; Zhushma, A. P.; Dobrynin, A. V.; Sheiko, S. S. Programming Temporal Shapeshifting. *Nat. Commun.* **2016**, *7* (May), 1–7.

(35) Dong, J.; Ozaki, Y.; Nakashima, K. Infrared, Raman, and Near-Infrared Spectroscopic Evidence for the Coexistence of Various Hydrogen-Bond Forms in Poly(Acrylic Acid). *Macromolecules* **1997**, *30* (4), 1111–1117.

(36) Sun, J.-Y.; Zhao, X.; Illeperuma, W. R. K.; Chaudhuri, O.; Oh, K. H.; Mooney, D. J.; Vlassak, J. J.; Suo, Z. Highly Stretchable and Tough Hydrogels. *Nature* **2012**, *489* (7414), 133–136.

(37) Haque, M. A.; Kurokawa, T.; Kamita, G.; Gong, J. P. Lamellar Bilayers as Reversible Sacrificial Bonds to Toughen Hydrogel: Hysteresis, Self-Recovery, Fatigue Resistance, and Crack Blunting. *Macromolecules* **2011**, *44* (22), 8916–8924.

(38) Tuncaboylu, D. C.; Sari, M.; Oppermann, W.; Okay, O. Tough and Self-Healing Hydrogels Formed via Hydrophobic Interactions. *Macromolecules* **2011**, *44* (12), 4997–5005.

(39) McCoul, D.; Hu, W.; Gao, M.; Mehta, V.; Pei, Q. Recent Advances in Stretchable and Transparent Electronic Materials. *Adv. Electron. Mater.* **2016**, *2* (5), 1500407.

(40) Trung, T. Q.; Lee, N. E. Recent Progress on Stretchable Electronic Devices with Intrinsically Stretchable Components. *Adv. Mater.* **2017**, *29* (3).

(41) Bauer, S.; Bauer-Gogonea, S.; Graz, I.; Kaltenbrunner, M.; Keplinger, C.; Schwödiauer, R. 25th Anniversary Article: A Soft Future: From Robots and Sensor Skin to Energy Harvesters. *Adv. Mater.* **2014**, *26* (1), 149–162.

(42) Hu, H.; Bhowmik, P.; Zhao, B.; Hamon, M. A.; Itkis, M. E.; Haddon, R. C. Determination of the Acidic Sites of Purified Single-Walled Carbon Nanotubes by Acid-Base Titration. *Chem. Phys. Lett.* **2001**, *345* (1–2), 25–28.

(43) Zhang, Y.; Xu, S.; Fu, H.; Lee, J.; Su, J.; Hwang, K.-C.; Rogers, J. A.; Huang, Y. Buckling in Serpentine Microstructures and Applications in Elastomer-Supported Ultra-Stretchable Electronics with High Areal Coverage. *Soft Matter* **2013**, *9* (33), 8062.

(44) Li, T.; Suo, Z.; Lacour, S. P.; Wagner, S. Compliant Thin Film Patterns of Stiff Materials as Platforms for Stretchable Electronics. *J. Mater. Res.* **2005**, *20* (12), 3274–3277.

(45) Gonzalez, M.; Axisa, F.; Bulcke, M. Vanden; Brosteaux, D.; Vandevelde, B.; Vanfleteren, J. Design of Metal Interconnects for Stretchable Electronic Circuits. *Microelectron. Reliab.* **2008**, *48* (6), 825–832.

(46) Lu, N.; Lu, C.; Yang, S.; Rogers, J. Highly Sensitive Skin-Mountable Strain Gauges Based Entirely on Elastomers. *Adv. Funct. Mater.* **2012**, *22* (19), 4044–4050.

(47) Gutruf, P.; Walia, S.; Nur Ali, M.; Sriram, S.; Bhaskaran, M. Strain Response of Stretchable Micro-Electrodes: Controlling Sensitivity with Serpentine Designs and Encapsulation. *Appl. Phys. Lett.* **2014**, *104* (2), 1–5.

(48) Li, Y.; Zhang, Z.; Li, X.; Zhang, J.; Lou, H.; Shi, X.; Cheng, X.; Peng, H. A Smart, Stretchable Resistive Heater Textile. *J. Mater. Chem. C* **2017**, *5* (1), 41–46.

(49) Kang, J.; Kim, H.; Kim, K. S.; Lee, S.-K.; Bae, S.; Ahn, J.-H.; Kim, Y.; Choi, J.; Hong, B. H. High-Performance Graphene-Based Transparent Flexible Heaters. *Nano Lett.* **2011**, 5154–5158.

(50) Li, Y. Q.; Zhu, W. Bin; Yu, X. G.; Huang, P.; Fu, S. Y.; Hu, N.; Liao, K. Multifunctional Wearable Device Based on Flexible and Conductive Carbon Sponge/Polydimethylsiloxane Composite. *ACS Appl. Mater. Interfaces* **2016**, *8* (48), 33189–33196.

(51) Zhou, R.; Li, P.; Fan, Z.; Du, D.; Ouyang, J. Stretchable Heaters with Composites of an Intrinsically Conductive Polymer, Reduced Graphene Oxide and an Elastomer for Wearable Thermotherapy. *J. Mater. Chem. C* **2017**, *5*, 1544–1551.

(52) Yoon, S. S.; Khang, D. Y. Facile Patterning of Ag Nanowires Network by Micro-Contact Printing of Siloxane. *ACS Appl. Mater. Interfaces* **2016**, *8* (35), 23236–23243.

(53) Hong, S.; Lee, H.; Lee, J.; Kwon, J.; Han, S.; Suh, Y. D.; Cho, H.; Shin, J.; Yeo, J.; Ko, S. H. Highly Stretchable and Transparent Metal Nanowire Heater for Wearable Electronics Applications. *Adv. Mater.* **2015**, *27* (32), 4744–4751.

(54) Hu, H.; Wang, Z.; Ye, Q.; He, J.; Nie, X.; He, G.; Song, C.; Shang, W.; Wu, J.; Tao, P.; Deng, T. Substrateless Welding of Self-Assembled Silver Nanowires at Air/Water Interface. *ACS Appl. Mater. Interfaces* **2016**, *8* (31), 20483–20490.

(55) Choi, S.; Park, J.; Hyun, W.; Kim, J.; Kim, J.; Lee, Y. B.; Song, C.; Hwang, H. J.; Kim, J. H.; Hyeon,

T.; Kim, D. H. Stretchable Heater Using Ligand-Exchanged Silver Nanowire Nanocomposite for Wearable Articular Thermotherapy. *ACS Nano* **2015**, *9* (6), 6626–6633.

(56) Ko, E.-H.; Kim, H.-J.; Lee, S.-M.; Kim, T.-W.; Kim, H.-K. Stretchable Ag Electrodes with Mechanically Tunable Optical Transmittance on Wavy-Patterned PDMS Substrates. *Sci. Rep.* **2017**, *7* (March), 46739.

(57) Jo, H. S.; An, S.; Lee, J.-G.; Park, H. G.; Al-Deyab, S. S.; Yarin, A. L.; Yoon, S. S. Highly Flexible, Stretchable, Patternable, Transparent Copper Fiber Heater on a Complex 3D Surface. *NPG Asia Mater.* **2017**, *9* (2), e347.

(58) Li, P.; Ma, J.; Xu, H.; Xue, X.; Liu, Y. Highly Stable Copper Wire/Alumina/Polyimide Composite Films for Stretchable and Transparent Heaters. *J. Mater. Chem. C* **2016**, *4* (16), 3581–3591.

(59) Ding, S.; Jiu, J.; Gao, Y.; Tian, Y.; Araki, T.; Sugahara, T.; Nagao, S.; Nogi, M.; Koga, H.; Suganuma, K.; Uchida, H. One-Step Fabrication of Stretchable Copper Nanowire Conductors by a Fast Photonic Sintering Technique and Its Application in Wearable Devices. *ACS Appl. Mater. Interfaces* **2016**, *8* (9), 6190–6199.

(60) An, B. W.; Gwak, E. J.; Kim, K.; Kim, Y. C.; Jang, J.; Kim, J. Y.; Park, J. U. Stretchable, Transparent Electrodes as Wearable Heaters Using Nanotrough Networks of Metallic Glasses with Superior Mechanical Properties and Thermal Stability. *Nano Lett.* **2016**, *16* (1), 471–478.

(61) Yeon, C.; Kim, G.; Lim, J. W.; Yun, S. J. Highly Conductive PEDOT:PSS Treated by Sodium Dodecyl Sulfate for Stretchable Fabric Heaters. *RSC Adv.* **2017**, *7* (10), 5888–5897.

ABSTRACT GRAPHIC

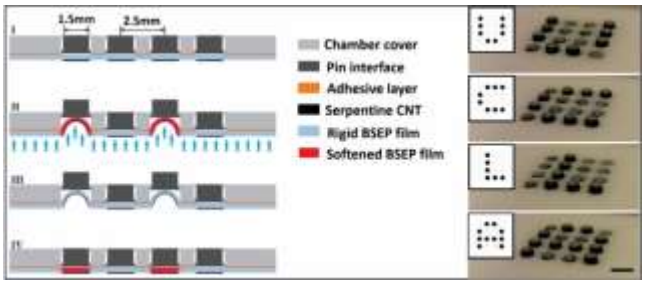

Supporting Information

Refreshable Tactile Display Based on a Bistable Electroactive Polymer and Stretchable Serpentine Joule Heating Electrode

*Yu Qiu, Zhiyun Lu, and Qibing Pei**

Department of Materials Science and Engineering, Henry Samueli School of Engineering and Applied Science, University of California, Los Angeles, CA 90095, USA

*Correspondence to: qpei@seas.ucla.edu.

Finite element analysis simulation:

Finite element analysis (FEA) was carried out to study the mechanical performances of BS80-AA5 thin film. By taking advantage of mathematical approximation, FEA could simplify the complex physical analysis process to the overall consideration of every discrete, small, simple but interactional element in the system. Through comparing the experimental results and the simulated results, a more accurate perception could be earned.

To better understand the actuation performances, a computer simulation based on ANSYS FEA software was performed. Like most elastomers, softened BSEP is essentially incompressible. The strain energy function W, which is the energy preserved in material per unit volume, is defined as:

$$W = \sum_{i=1}^{N} C_{i0}(\overline{I_1} - 3)^i \quad (5)$$

Where:

W = The strain energy density, which is strain per unit volume;

N = A positive deciding the number of terms in the above function (N=1 for Yeoh's 1st model, N=2 for Yeoh's 2nd model and N=3 for Yeoh's 3rd model);

$\overline{I_1}$ = The first invariant of the deviatoric strain;

C_{ij} = Material constants, describing the shear behavior of the material;

By fitting the strain energy density function with the experimental uniaxial stress-strain curve (Figure S5) through nonlinear least square optimization technique, Yeoh's 3rd hyperelastic model was selected to tailor the mechanical properties of softened BS80-AA5. Thus, the strain energy density function W was determined as:

$$W = 75060(\overline{I_1} - 3) + 22284(\overline{I_1} - 3)^2 - 908.2(\overline{I_1} - 3)^3$$

The constants in this nonlinear elastic model were derived from the strain-stress curve measured from the experimental uniaxial tensile test. Solid 185, a three-dimensional eight-node element type, was used to mesh the model. Besides, for the solver control of the FEA process, the large deflection option was on to take the nonlinear effect in for consideration. The model was set according to the international Braille standard. For the reported 4 × 4 tactile display, a layer of BS80-AA5 was first created on the bottom, on top of which a rigid PMMA substrate with through holes that correspond with the taxel areas was glued. In this way, areas other than the taxels are all constrained by the PMMA board as fixed support to prevent any deformation.

Demonstration of actuation:

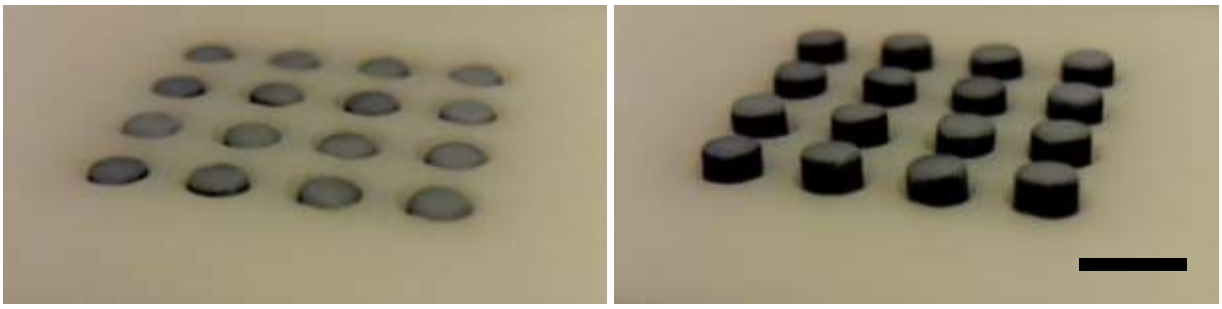

Figure S1. Photographs of a 4 × 4 tactile display in the flat state (left) and all actuated state (right). Both states are stable without any external energy input. The scale bar represents 2 mm.

The left image of Figure S1 shows the 4 × 4 tactile display in the "OFF" state when the BSEP film was not deformed and the surface of the display was flat. The right image shows that all the taxels were actuated with a stroke of 0.7 mm. Both two states are stable without any external energy input.

Bistable mechanism of BSEP material:

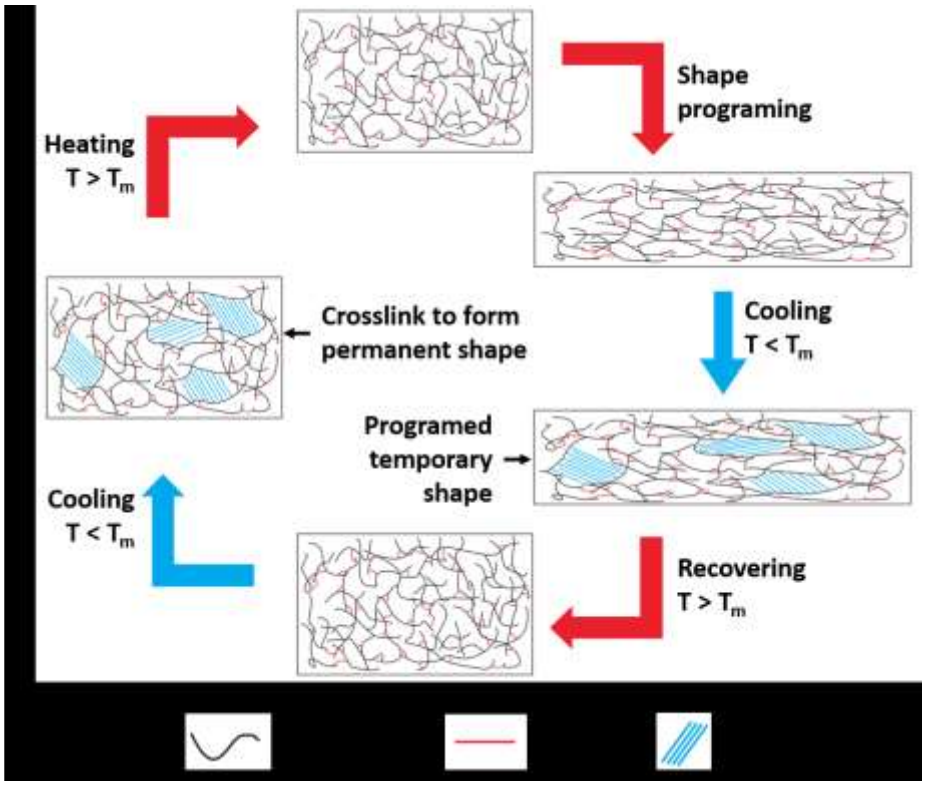

Figure S2. Schematic illustration of shape memory mechanism of phase changing BSEP.

The BSEP material is a variable stiffness polymer comprising nanometer-size crystalline aggregates in a chemically crosslinked polymer matrix. The shape memory property is obtained by reversible crystal melting (phase-changing), resulting in a material with large modulus change between the rigid and rubbery states during temperature cycles. Below its transition temperature, the soft side chains (SA moieties) from different polymer backbones pack closely to form crystalline aggregates which stiffen the material. Above the melting temperature (T_m) of the crystalline aggregates, the polymer becomes rubbery and can be programed into different shapes. Such deformation may be preserved by cooling down the temperature below T_m as the crystalline

aggregates of SA moieties reform. And the shape can be recovered by reheating the polymer above T_m.

BS80-AA5 composition:

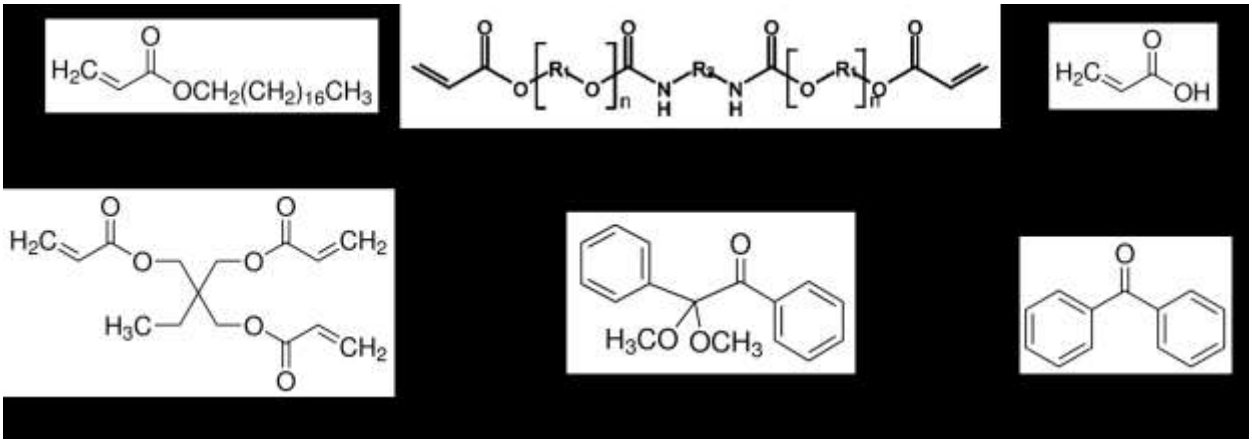

Figure S3. Chemical structures of monomers and initiators used for the synthesis of S80-AA5.

For an idea BSEP based tactile actuator, large blocking force, low actuation (pneumatic) pressure, and high mechanical toughness are the main aspects that are needed to be considered. Stearyl acrylate (SA) has a long alkyl chain that can crystallize at room temperature. The reversibly crystallizing and melting of SA moieties provide the variable stiffness property. Urethane diacrylate (UDA) is an oligomer comprising flexible polyether diol segments. UDA was selected as long chain crosslinker to enhance elongation at break and improve the toughness. Trimethylolpropane triacrylate (TMPTA), which is a trifunctional acrylic monomer, was used as small molecule corsslinker to provide the network baseline. Such small molecule crosslinker can stiffen the polymer at larger strains, thus increase the tensile strength. Acrylic acid (AA) was added to introduce hydrogen bonds to the polymer system, which can help increase the modulus change,

mechanical toughness, and electrode bonding. 2,2-Dimethoxy-2-phenylacetophenone (DMPA) and benzophenone (BP) were synergistically used as co-initiators to achieve complete bulk and surface curing in thin films.

Shape memory demonstration:

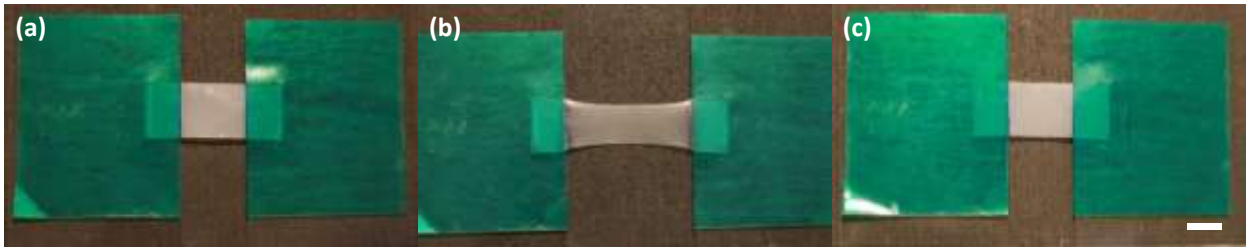

Figure S4. Shape memory demonstration of a BS80-AA5 film at its original shape (a), deformed with 100% linear strain via a heating-stretching-cooling procedure (b), and recovered to original shape (c). All shapes are rigid and free-standing. The scale bar represents 1 cm.

The shape memory property was demonstrated in Figure S4. A strip made from BS80-AA5 was attached on two pieces of Kapton^{TM} tape at the ends (Figure S4a). The initial distance between two tapes was 1.5 cm. At 50 ^{o}C, the softened BS80-AA5 was stretched to 3 cm with a linear strain of 100%. The film was then cooled down in air to "lock" the deformation. The deformed film was free-standing with a fixation rate close to 100% (Figure S4b). The original shape can be recovered by heating the strip again above the transition temperature, and the recovery rate is 100% (Figure S4c).

Tensile test measurement:

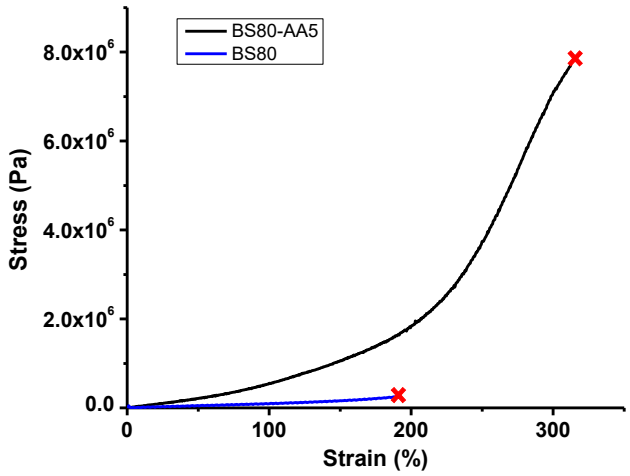

Figure S5. Tensile stress-strain response of BS80-AA5 and BS80 at 50 ºC. The stretching rate is 0.1 mm/s.

The tensile stress-strain response of softened BS80-AA5 and BS80 were measured at 50 ºC using DMA. The tensile strength is 7.73 MPa for BS80-AA5 and 0.26 MPa for BS80, while the elongation at break is 320% and 191% for BS80-AA5 and BS80 respectively. The improved toughness of BS80-AA5 is due to the reversible crosslinks introduced by acrylic acid.

BS80-AA5/Poly(UDA) mechanical tests:

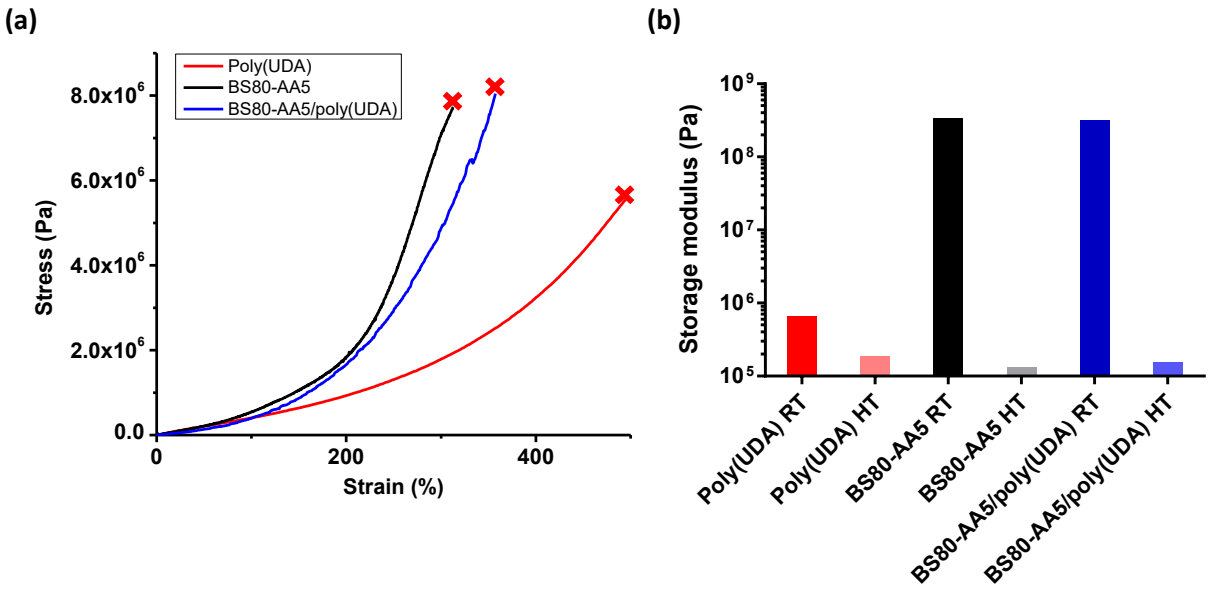

Figure S6. (**a**) Tensile test comparison of poly(UDA), BS80-AA5, and BS80-AA5/poly(UDA) composite. The composite film was made by spraying and curing a thin layer of poly(UDA) (5 µm) on a 90 µm BS80-AA5; (**b**) Storage modulus measurements of the three materials at room temperature (RT) and 50 ºC high temperature (HT).

UDA is a urethane diacrylate oligomer comprising a flexible polyether diol segment and an aliphatic diisocyanate segment. The homopolymer, poly(UDA), has a large elongation at break of 495%, a tensile strength of 0.93 MPa, and a modestly low modulus of 0.66 MPa at room temperature and 0.19MPa at 50 ^{o}C. The resulting BS80-AA5/poly(UDA) composite film has higher maximum elongation of 357% and tensile strength of 8.05 MPa compare to pristine BS80-AA5. Despite the strengthening effect from poly(UDA), the stress-strain behavior of the two films are very similar at strain smaller than 200%. Thus poly(UDA) won't have much mechanical effect on the BSEP film during operation of the device. At room temperature, because of the lower modulus of poly(UDA), the storage modulus of the composite film is lower (320 MPa) compare to that of BS80-AA5 (344 MPa). In the rubbery state, the composite possesses a slightly higher modulus of 0.16 MPa compare to 0.13 MPa of BS80-AA5.

Pneumatic pressure measurement:

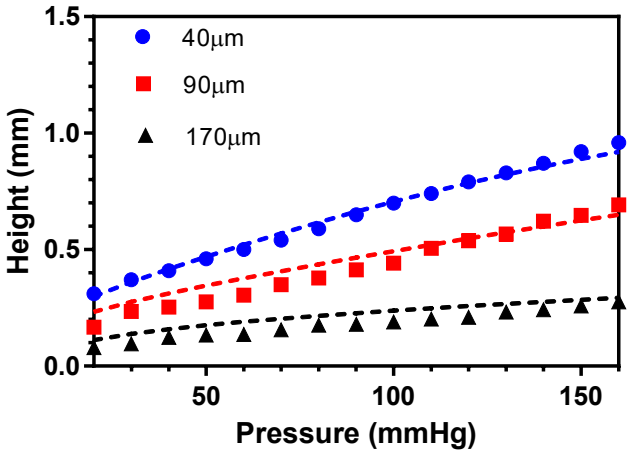

Figure S7. Measured (symbols) and simulated (dashed curves) internal air pressure needed to actuate a softened BSEP taxel to different heights. The thickness of the BSEP films ranges from 40 μm to 170 μm.

To demonstrate the easy actuation, ANSYS finite element model was carried out to simulate the internal pneumatic pressure needed to actuate a taxel to different heights. The tests were conducted on BS80-AA5 film with thickness ranging from 40 μm to 170 μm. The simulated results match the experimental data quite well. The pneumatic pressure to generate a stroke of 0.7 mm is 100 mmHg for 40 μm BSEP and 160 mmHg for 90 μm BSEP. For the 170 μm BSEP, the stroke with 160 mmHg pressure is only 0.3 mm. The thinner the BSEP film is, the lower pressure it is required to actuate the taxel to the same height. However, if the BSEP is too thin, the taxel may not be able to provide enough blocking force to the end user. Thus, 90 μm BSEP was chose to fabricate the tactile display. Please note that 160 mmHg is not high pressure, as a latex balloon in its 2/3 capacity has a pressure of 810 mmHg.

Electrode-substrate bonding test:

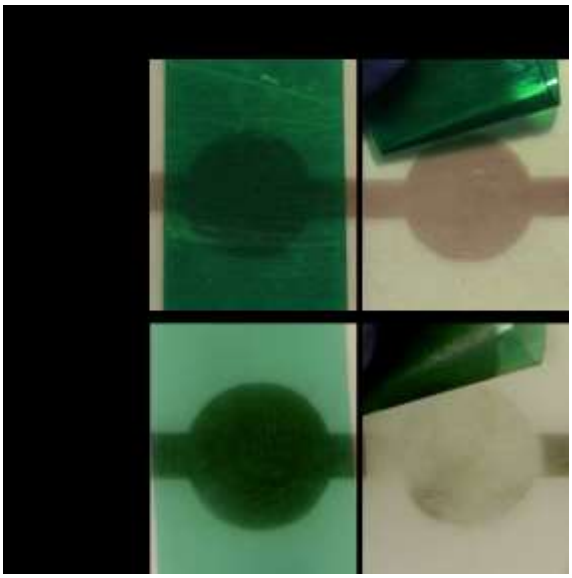

Figure S8. Testing of the adhesion of CNT on BS80-AA5 and BS80 film using Kapton™ tape.

Figure S8 shows the adhesion tests of CNT electrode on BSEP substrates. Same amount of CNT solution was sprayed on BS80-AA5 and BS80 respectively through a shadow mask. The resulting CNT/BS80-AA5 and CNT/BS80 has the same initial resistance. Two pieces of Kapton™ tape with peeling strength of 46 oz/in were attached firmly on top of CNT/BSEPs. The tapes were then peeled off, and the resistance of the electrodes were measured subsequently. The results show a constant resistance of CNT/BS80-AA5 after 3 repetitive tape-peel tests, while CNT/BS80 lost surface conductivity after one test as almost all the CNT has transferred to the tape. The results demonstrate the strong bonding between CNT and BS80-AA5, and such strong bonding is because of the hydrogen bond interaction between acrylic acid and SWNT-COOH.

Serpentine and round shaped electrode comparison:

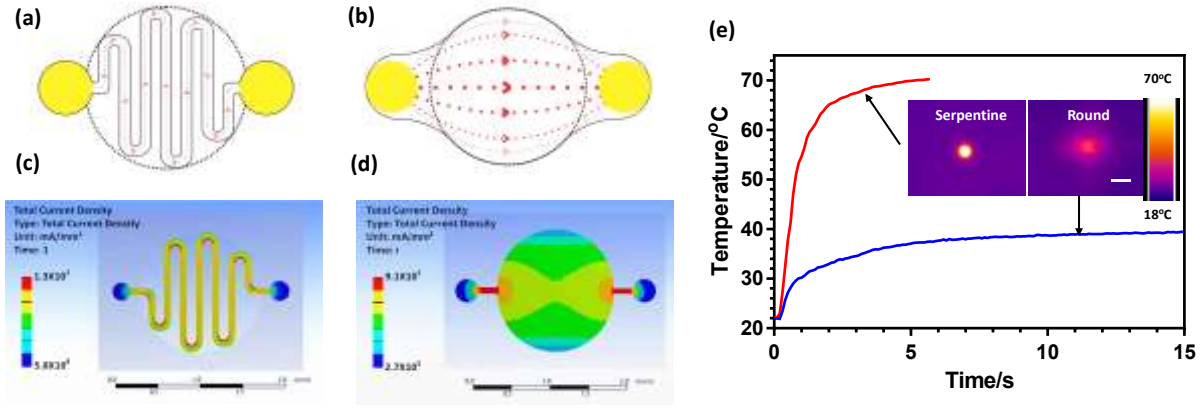

Figure S9. Illustration (**a,b**) and simulated (**c,d**) results of current density distribution in serpentine shaped and round shaped electrodes. The widths of the red dotted lines in (**a**) and (**b**) indicate relative current density. (**e**) Transient temperature responses of the electrodes at 30 V. Insets in (**e**) are infrared camera images of the heated electrode areas. The scale bar is 2 mm.

To demonstrate the heating performance, ANSYS finite element analysis was also carried out to simulate the current density distribution in serpentine shaped and round shaped electrode. (Figure S9a) Both models are established according to the setup of one taxel. The resistivity of SWCNT (10^{-7} Ω·m) and the mesh size of 0.02 mm were applied to the two models. 30 V was set as the activation voltage during the simulation. The serpentine shaped and round shaped electrode were divided into 6578 elements and 3103 elements respectively to analyze their steady-state electric conduction. Based on the simulation results, serpentine shaped CNT has a more uniform distribution of current density within the electrode area, which should serve better as heating electrode.

The experimental results of the heating performance of serpentine shaped CNT and round shaped CNT are also corresponding with the simulation. (Figure S9b) With same resistance (50 kΩ) and

voltage supply (30 V), serpentine shaped electrode exhibits higher and more locally defined heating spots. For the S-CNT, the time needed to reach 50 ºC, which is the temperature to soften BS80-AA5, is less than 1 s whereas round shaped electrode is unable to reach the required temperature even after 5 seconds of applied voltage. The infrared thermal images (ICI 9320P) of the serpentine shaped electrode illustrates these advantages. That is because that during the lengthy heating process of round shaped electrode, more and more heat dissipates through air and surrounding materials, crosstalk of adjacent taxels could happen with such high-density array. As for serpentine shaped CNT, the unique winding path increases the heating efficiency, result in rapid heating in a very short time.

Joule heating characterization of S-CNT:

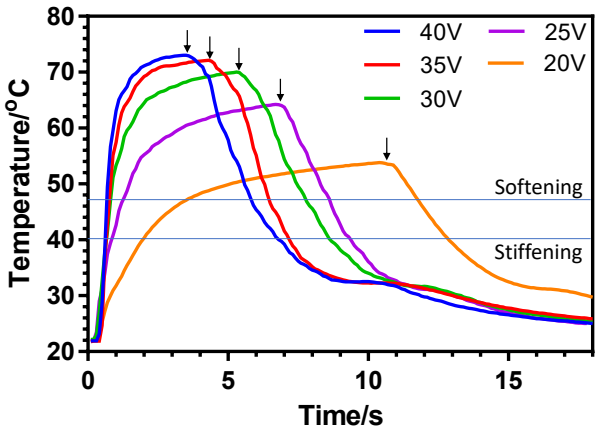

Figure S10. Temperature profiles of S-CNT electrode under different voltage supplied. Downward arrows indicate when heating voltage is removed. The "Softening" line indicate the temperature above which the polymer is soft, and the "Stiffening" line the temperature below which the polymer is stiff.

Figure S10 shows the time evolution of temperature increase and decrease for the serpentine CNT electrode under different voltage input. The temperature increased rapidly with time and reached a relative saturated plateau. The plateau increased with the input power. In most cases, the taxel can reach the softening line, which is 47 °C, within a few seconds. The cooling process takes longer because of the temperature overshooting. For the proposed taxel, 40 °C is the temperature to stiffen the material, so the cooling time usually takes less than 2 s.

Thermal and pneumatic control sequence:

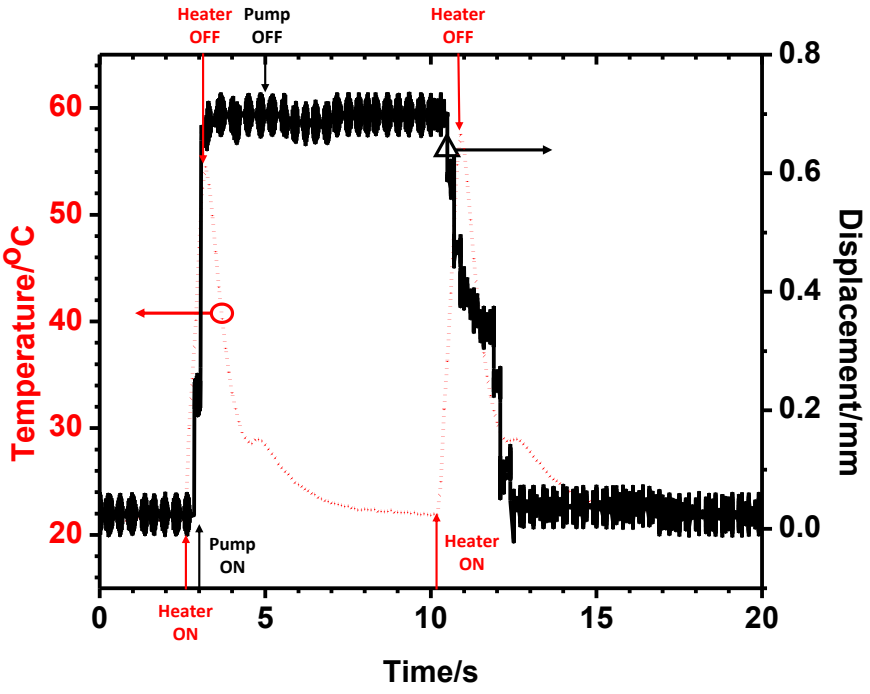

Figure S11. Raised height and temperature of a taxel as a function of time during a bistable actuation cycle.

Figure S11 demonstrates the thermal and pneumatic control sequence of a taxel. The actuation cycle starts with the BS80-AA5 membrane at room temperature and in an OFF state. The interface surface is flat. The taxel area of BS80-AA5 is heated up by S-CNT Joule heating electrode for 1 s. Then the pneumatic pump is turned on with the S-CNT electrode voltage removed at the same time. The softened BSEP area is deformed out-of-plane by the pneumatic pressure, which props up the pin interface. The taxel is allowed to cool for 2 s before the pump is turned off. The raised

pin’s height is measured to be around 0.7 mm and remains relative stable after removal of the internal pneumatic pressure. The raised pin falls back to the original position when the deformed BS80-AA5 is softened by the Joule heating electrode and recovers to flat.